Somes applications of B-Spline functions in Image Processing

A. Diou, Y. Voisin, L.F.C. Lew Yan Voon, G. Moreels*, J. Clairemidi*
Laboratoire Le2i, Université de Bourgogne
12, rue de la fonderie
F-71200 Le Creusot, FRANCE
Tel: (33)-3-85-73-10-44 ; Fax:(33)-3-85-73-10-99, E-mail: a.diou@iutlecreusot.u-bourgogne.fr
* Observatoire de BESANCON

Abstract

A digital image is the result of spatial sampling of an image formed in a naturally continuous way by the optical shooting system. A certain amount of information is masked by the sampling process when it is not purely removed by the latter (for example all the information in the initial continuous image which do not satisfy the Shannon theorem). B-Spline functions are one of the means of transforming a digital image into a continuous image, knowing that it would not be possible to restore the information lost during sampling. We present herein some applications of B-Spline functions in image processing, particularly in interpolation and zooming, edge detection, multiresolution analysis applied to the equalization of the background of an image, and the analysis of ground topography.

1 Decomposition of an image into B-Spline functions

1.1 B-Spline Functions

They are piecewise continuous functions, composed of polynomials, defined on a bounded support [5]. Each piece of continuous function is defined over an interval of unit width. The number of pieces depends on the order of the spline. The p-order B-Spline (B_p) is composed of $(p+1)$ polynomials of degree p. It is defined over the interval $x \in [-(p+1)/2, (p+1)/2]$.

The 0-order B-Spline is the "windows" function defined over the interval $x \in [-1/2, +1/2]$. Each B-Spline is obtained by the recurrent equation [8]:

$$B_p(x) = B_{p-1}(x) * B_0(x),$$

which allow to make explicit the function :

$$B_p(x) = \sum_{j=0}^{p+1} \frac{(-1)^j}{p!} C_{p+1}^j \left(x + \frac{p+1}{2} - j\right)^p \times \mu\left(x + \frac{p+1}{2} - j\right)$$

{*where* $\mu(x)$ *is the Heaviside function*}. B-Spline functions up to order 5 are plotted in figure 1 :

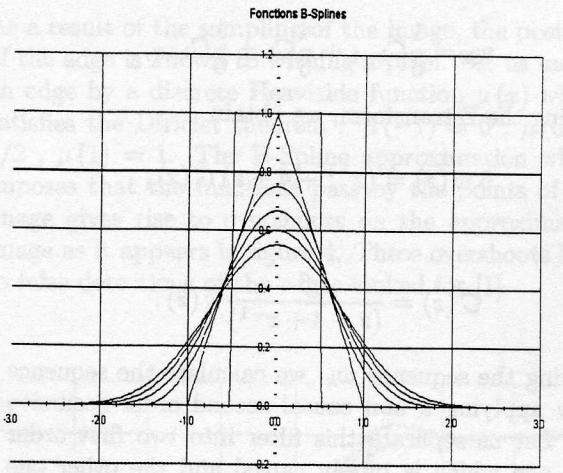

Figure 1: B-Spline functions up to order 5

1.2 Decomposition algorithme

1.2.1 One-dimensional signal

Let w_k be the gray value of pixel k. k takes the whole values of the x-axis for $x \in [-1/2, K-1/2]$, where K is the number of pixels.

The interpolated function is

$$w(x) = \sum_{j=0}^{K-1} C_j B_p(x-j).$$

This function is such that

$$w_k = w(k) = \sum_{j=0}^{K-1} C_j B_p(k-j).$$

However, the B_p are null outside a certain interval, which means that the sum is over a limited number of terms. Among all the splines, cubic splines are very often used because the polynomials are of degree 3 which is high enough for a good interpolation (continuity of order 2), and not too high so that the complexity is maintained at a reasonable level.

Calculating the C_k We would like to approximate the grey value by :

$$w(x) = \sum_{j=0}^{K-1} C_j B_3(x-j),$$

such that $w(x) = w_k$ when $x = k$. It thus results

$$w_k = \frac{1}{6}C_{k-1} + \frac{4}{6}C_k + \frac{1}{6}C_{k+1},$$

Using the Z-transform, we obtain

$$6\,w(z) = \left(z^{-1} + 4 + z\right) C(z),$$

or

$$C(z) = \frac{6}{(z+4+z^{-1})} w(z).$$

Knowing the sequence w_k, we calculate the sequence C_k by applying a non causal second order recursive filter. Let us separate this filter into two first order filter, one which is purely causal and the other one purely anti-causal. Only the pole of modulus less than one that is to say $\alpha = -2 + \sqrt{3}$ is kept.[10][11] So,

$$C(z) = \frac{\alpha - 1}{z - \alpha} \times \frac{\alpha - 1}{z^{-1} - \alpha} w(z).$$

Denoting the causal part by C^+ it becomes

$$C^+(z) = \frac{1-\alpha}{z-\alpha} w(z)$$

$$C(z) = \frac{1-\alpha}{z^{-1}-\alpha} C^+(z)$$

Let us calculate the recurrent relations. For the causal part :

$$C^+_{k+1} = w_k - \alpha(w_k - C^+_k) \; \{forward\ iteration\}.$$

For the anti-causal part :

$$C_{k-1} = C^+_k - \alpha(C^+_k - C_k) \; \{backward\ itération\}.$$

1.2.2 Two-dimensional signal

Let us consider an image of dimension $L \times K$. It will be decomposed in a separable way firstly in lines, then in columns :

$$w(x,y) = \sum_{i=0}^{L-1} \sum_{j=0}^{K-1} D_{ij} B_3(y-i) B_3(x-j), \quad (1)$$

The grey values are known at coordinates ($x = k, y = l$). The decomposition is done in two steps, firstly by calculating the coefficients C_{ik} from the grey values

$$w(k,l) = \sum_{i=0}^{L-1} C_{ik} B_3(l-i),$$

then the coefficients D_{ij} from the C_{ik}

$$C_{ik} = \sum_{j=0}^{K-1} D_{ij} B_3(k-j).$$

The algorithms are identical to those used in the one-dimensional case.

2 Application examples

2.1 Search for edges and extrema.

One of the definitions of an edge is the locus of points where the modulus of the gradient is maximal. An extrema is the locus of points where the gradient is null. Let us consider the gradient image $G(x,y)$ formed from the image $w(x,y)$:

$$G(x,y) = \sqrt{\left(\frac{\partial w(x,y)}{\partial x}\right)^2 + \left(\frac{\partial w(x,y)}{\partial y}\right)^2}$$

The differential operator cannot be applied directly on the discrete image, however, they can be applied

on the continuous image obtained by the B-Spline approximation, that is to say

$$G(x,y) = \sqrt{\left(\sum_{i=0}^{L-1}\sum_{j=0}^{K-1} D_{ij} B_3(y-i)\,\frac{\partial B_3}{\partial x}(x-j)\right)^2 + \left(\sum_{i=0}^{L-1}\sum_{j=0}^{K-1} D_{ij} B_3(x-j)\,\frac{\partial B_3}{\partial y}(y-i)\right)^2},$$

or for instance at coordiantes $x = k, y = l$:

$$G(k,l) = \sqrt{\left(\frac{D_{l+1,k+1} - D_{l+1,k-1} + D_{l-1,k+1} - D_{l-1,k-1}}{12}\right)^2 + \left(\frac{D_{l+1,k+1} + D_{l+1,k-1} - D_{l-1,k+1} - D_{l-1,k-1}}{12}\right)^2}.$$

2.1.1 An exemple on the image of the comet HYAKUTAKE

Two of us have taken the image of the comet HYAKUTAKE (figure 2). The dimension of this image is 512×512 pixels, each pixel represents a surface area of $70km \times 70km$. Compression waves due to the pressure of the sun radiation were looked for in the tail. These compression waves were brought to the fore in the gradient image, followed by an enhancement of the low grey values. The processed image show in addition the rotation of the core of the comet (figure 3).

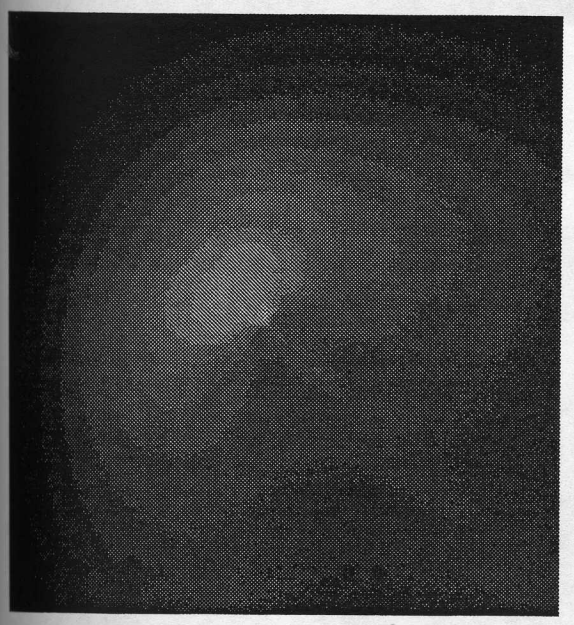

Figure 2: Comet HYAKUTAKE, image taken by G. Moreels and J. Clairemidi, Observatory of BESANCON

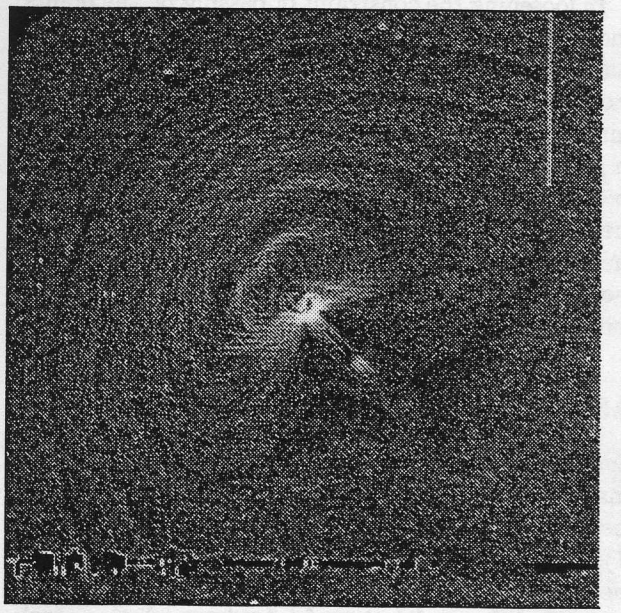

Figure 3: Gradient image of the comet HYAKUTAKE

2.2 Discussion on the edge detection

As a result of the sampling of the image, the position of the edge is known to withing a pixel. Let us model an edge by a discrete Heaviside function $\mu(x)$ which satisfies the Diriclet theorem : $\mu(-1) = 0$, $\mu(0) = 1/2$, $\mu(1) = 1$. The B-Spline approximation which imposes that the functions pass by the points of the image gives rise to overshoots on the approximated image as it appears in figure 4. These overshoots lead to false detections of the edges looked for [1].

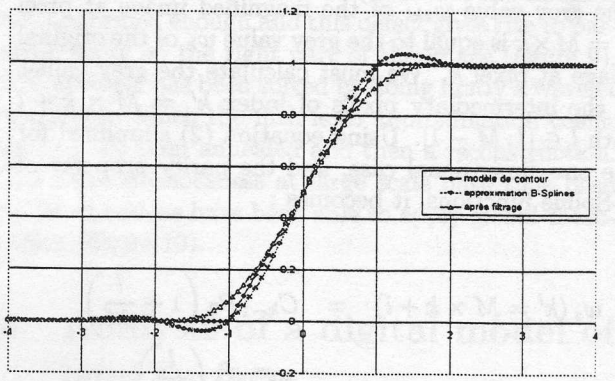

Figure 4: Approximation of the step function

In loosening the constraint of passing by the points, and nevertheless in trying to obtain a curve which matches at best the step function model without overshoot, we show that we only need to filter the original image by a filter of the form $F(z) = \frac{1}{6}\left(z^{-1} + 4 + z\right)$. In fact, this filter is the inverse filter of the one used to calculate the coefficients C_k of the development of the image in B-Spline functions.The coefficients C_{fk} of the development of the filtered image is nothing but the grey values : $C_{fk} = w_k$. The approximation of the contour after filtering is given in figure 4.

2.3 Interpolation

Having at our disposal a continuous description of the image, it is possible to detremine the grey value of the image for any none integer coodinate by applying (1). The functions $B_3(x)$ being equal to zero outside the interval $x \in [-2, 2]$, the calculation of $w(x, y)$ is reduced to the application of a 4×4 convolution mask on the D_{ij} coefficient image :

$$
\begin{aligned}
& w(k + \Delta x, l + \Delta y) \qquad (2) \\
= & \sum_{i=l-1}^{l+2} \sum_{j=k-1}^{k+2} D_{ij} B_3(l - i + \Delta y)\, B_3(k - j + \Delta x) \\
= & \sum_{i=-1}^{2} \sum_{j=-1}^{2} D_{i+l,j+k} B_3(-i + \Delta y)\, B_3(-j + \Delta x)
\end{aligned}
$$

2.4 Zooming

We would like to magnify an image by a factor M. Let us reason on a one-dimensional image, the extension to an two-dimensional image is straightforward as a result of the separability.The original image consist of K pixels, the magnified image consist of $M \times K$ pixels. The grey value $w_{zk'}$ of the magnified image at pixel $k' = M \times k$ is equal to the grey value w_k of the original image at pixel k. We must calculate the grey values of the intermediary pixels of index $k' = M \times k + l$ with $l \in [1, M - 1]$. Using equation (2) simplified for the one-dimensional case, and the parity property of B-Spline functions, it becomes :

$$
\begin{aligned}
w_z(k' = M \times k + l) \;=\; & C_{k-1} B_3\left(1 + \frac{l}{M}\right) \\
& + C_k B_3\left(\frac{l}{M}\right) \\
& + C_{k+1} B_3\left(1 - \frac{l}{M}\right) \\
& + C_{k+2} B_3\left(2 - \frac{l}{M}\right).
\end{aligned}
$$

If we use the filtered image in order to avoid overshoots during high grey value transitions, then the C_k are equal to the w_k.

2.4.1 An example on the image "Port of St Helier"

From the image of figure 5, we have selected a zone which is magnified by 4, see figure 6.

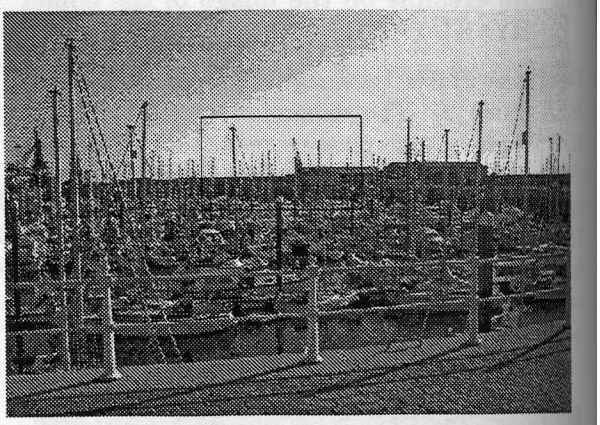

Figure 5: "Port of St Helier", original image

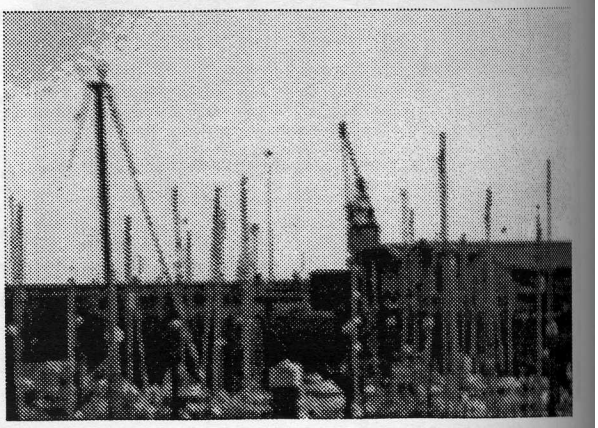

Figure 6: A piece of the image "Port of St Helier", magnified by 4

3 Multiresolution analysis

3.1 Wavelet transform

Wavelet transform consists in obtaining an approximation of a signal f by projecting this signal on an approximation space V_j using an operator A_j. Since this approximation leads to a lost of part of the information, the recontruction of the signal requires that an operator D_j, which projects the same signal on the detail space W_j, such that $A_{j-1}f = A_j f + D_j f$ [2][6] The approximation and the detail spaces are build from respectively the base functions $\varphi(x)$ and $\psi(x)$ which are obtained by recurrence by applying the digital filters $h[k]$ and $g[k]$. The analysis of a digital signal is done by applying filters $\widetilde{h}$ and $\widetilde{g}$ followed by a decimation of one term in every two. We obtain thus the approximation signal a^j and the detail signal d^j at the j^{th} resolution, the resolution $j = 0$ being the initial resolution. The reconstruction is done by over-sampling of factor 2 followed by the application of filters $\overline{h}$ et $\overline{g}$ and the sum of the two sequences. The algorithm of Mallat is given in figure 7 [7].

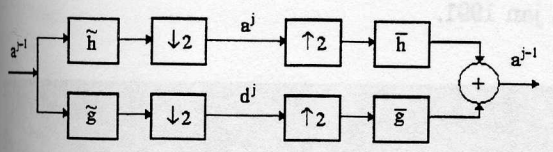

Figure 7: Mallat's algorithm, decomposition and reconstruction

3.2 Bi-orthogonal cubic B-Spline wavelets

Starting with the mother function $\varphi(x)$, we look for the wavelet function $\psi(x)$ which allows multiresolution analysis and which is such that it is orthogonal to $\varphi(x)$ [3][12]. This often leads to infinite impulse response filters h and g, which are truncated in order to ensure implementability. If we content ourself with the bi-orthogonality between $\varphi(x)$ and $\psi(x)$, then we can construct the filters h and g in the form of recursive filters with a low number of coefficients [4]. This is the case if we choose for $\varphi(x)$ a B-Spline function. The parity of these function implies that $\widetilde{h} = h$ and $\widetilde{g} = g$. In choosing the cubic B-Spline, the Z-transform of the filters after factorization is written as :

$$H(z) = \sqrt{2}\left(\frac{z^{-1}+1}{2}\right)\left(\frac{z^{-1}+1}{2}\right)\left(\frac{z+1}{2}\right)\left(\frac{z+1}{2}\right),$$

$$\begin{aligned} G(z) &= \sqrt{2}z\left(\frac{z^{-1}-1}{2}\right)\left(\frac{z^{-1}-1}{2}\right)\left(\frac{z-1}{2}\right)\left(\frac{z-1}{2}\right) \\ &\times \left(\frac{z^{-1}-\alpha}{z^{-2}+\alpha}\right)\left(\frac{z^{-1}-\beta}{z^{-2}+\beta}\right)\left(\frac{z^{-1}-\gamma}{z^{-2}+\gamma}\right) \\ &\times \left(\frac{z-\alpha}{z^2+\alpha}\right)\left(\frac{z-\beta}{z^2+\beta}\right)\left(\frac{z-\gamma}{z^2+\gamma}\right), \end{aligned}$$

$$\begin{aligned} \overline{H}(z) &= \sqrt{2}\left(\frac{z^{-1}+1}{2}\right)\left(\frac{z^{-1}+1}{2}\right)\left(\frac{z+1}{2}\right)\left(\frac{z+1}{2}\right) \\ &\times \left(\frac{z^{-1}+\alpha}{z^{-2}+\alpha}\right)\left(\frac{z^{-1}+\beta}{z^{-2}+\beta}\right)\left(\frac{z^{-1}+\gamma}{z^{-2}+\gamma}\right) \\ &\times \left(\frac{z+\alpha}{z^2+\alpha}\right)\left(\frac{z+\beta}{z^2+\beta}\right)\left(\frac{z+\gamma}{z^2+\gamma}\right), \end{aligned}$$

$$\overline{G}(z) = -z^{-1}\sqrt{2}\left(\frac{z^{-1}-1}{2}\right)\left(\frac{z^{-1}-1}{2}\right)\left(\frac{z-1}{2}\right)\left(\frac{z-1}{2}\right).$$

Three parameters only appear in these expressions : $\alpha = 0.5352804311, \beta = 0.12255461521, \gamma = 0.009148694851$.

3.3 Application to the uniformization of the background of an image

We have been asked to solve the problem of isolating and dimensioning corretly inclusions in steel. The inclusions appear in dark on a bright background (figure 8), it seemed easy to set them forth by a simple global thresholding on the image using the moment preserving method. However, the background of the image is not uniformed enough and this defect gives rise to parasitic spots on the right part of the image (figure 9). The problem has been solved by doing firstly a wavelet analysis in which the fifth level approximation coefficients have been annealed and then a reconstruction. The heterogeneousness at large scale have thus been removed and we have been able to apply global thesholding (figure 10).

4 Analysis of a digital model of land surface

A digital model of land surface is a two-dimensional file where the value stored represents the altitude of

the point under consideration. Having at our disposal the digital model of the land surface of the region "Jura" (France), we have transformed it into an image of 1024×512 pixels, where each pixel represents a land surface area of $75m \times 75m$ and where the grey value is proportionnal to the altitude (figure 11). We give in figure 12 a 3-D view of this region.

We have applied a multiresolution analysis up to the 7^{th} level of analysis in order to put forth land structures at different scales. The image of figures 13 and 14 have been reconstructed by keeping only the 7^{th} level approximation coefficients, those of figures 15 and 16, have been reconstructed by keeping the approximation and detail coefficients of level 6 to 4 and those of figures 17 and 18 have been reconstructed by keeping only detail coefficients of level 4 to level 1. We can see on these figures the structures at these different scales.

We presents herein only the results that we can obtain with this image processing tool, a team of geologist colleagues of the University of Burgundy ("Université de Bourgogne", France) to whom we have provided with this tool will take care of the interpretations of these results, and of the parametrization of this tool according to the structures looked for.

5 Conclusion and current work

B-Spline functions provide us with a very powerful analysis tool, easy to use, and fast. The algorithms being made up of recursive filters of first and second order, we are currently investigating their implementations in FPGA circuits in order to obtain real time processing operators [9].

6 References

[1] A. Chehikian, "Filtres récursifs pour l'estimation du gradient et la détection de contours par interpolation Spline", *Traitement du Signal*, Vol 14, N°1, pp. 29-42, 1997.

[2] I. Daubechies, "Ten Lectures on Wavelets", *SIAM*, Philadelphia,PA,1992

[3] I. Daubechies, Orthonormal bases of compactly supported wavelets", *Com. on Pure Appl. Math.*, Vol 41, pp. 919-996, Nov 1988

[4] B. Delyon, "Ondelettes orthogonales et biorthogonales", *Publication interne IRISA*, N°732, 1993.

[5] M. Eden, M. Unser, R. Leonardi, "Polynomial representation of picture", *Signal Processing*, Vol. 10, pp. 385-393, Jul. 1986.

[6] S. Mallat, "A theory for multiresolution signal decomposition : the wavelet representation", IEEE, *PAMI*, Vol. 11, N°7, pp. 674-693, Jul 1989.

[7] S. Mallat, "Multiresolution approximations and wavelet orthonormal bases of $L^2(R)$, *Trans. Am. Math. Soc.*, vol. 315, N°1, pp.69-87, Sep.1989

[8] H. Olkkonen, "Discrete Binomial Splines", *Graphical Models and Image Processing*, Vol. 57, N°2, pp. 101-106, 1995.

[9] F. Truchetet, A. Forys, "Implementation of still-image compression-decompression scheme on FPGA circuits", *Still image Compression*, SPIE, Vol. 2669, pp. 66-75, Jan 1996.

[10] M. Unser, A. Aldroubi, M. Eden, "B-Spline signal processing : part I - Theory", *IEEE Trans. on PAMI*, Vol. 41, N°2, pp. 821-832, 1993.

[11] M. Unser, A. Aldroubi, M. Eden, "B-Spline signal processing : part II - Efficient design and applications", *IEEE Trans. on PAMI*, Vol. 41, N°2, pp. 834-848, 1993.

[12] E. Viscito, J.P. Allebach, "The analysis and design of multidimensional FIR perfect reconstruction filter banks for arbitrary sampling lattices", *IEEE Trans. on Circuits and systems*, Vol 38, N°1, pp. 29-41, jan 1991.

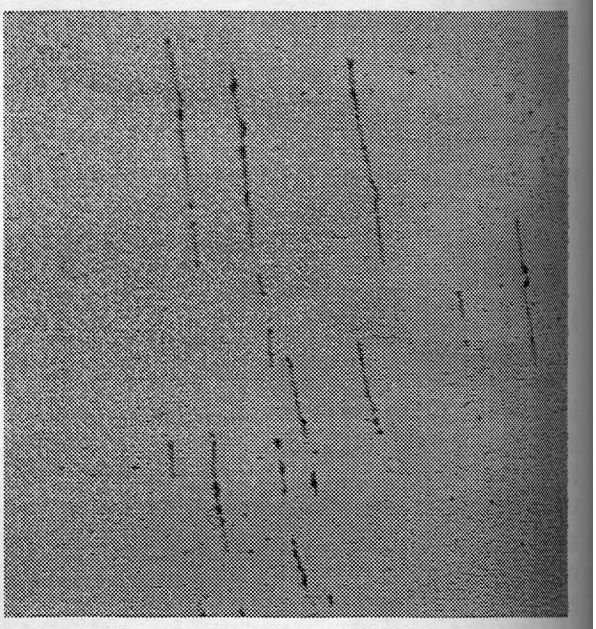

Figure 8: Inclusions in steel, raw image

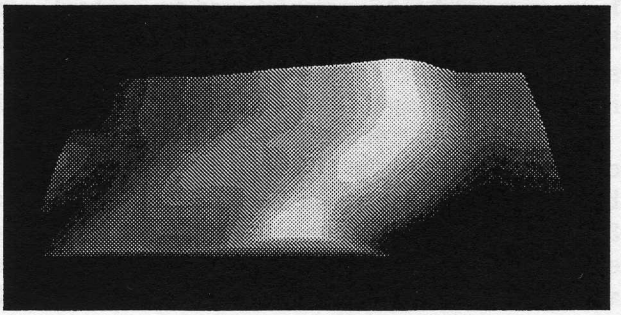

Figure 14: 3-D view of the 7th level approximation of image "Jura"

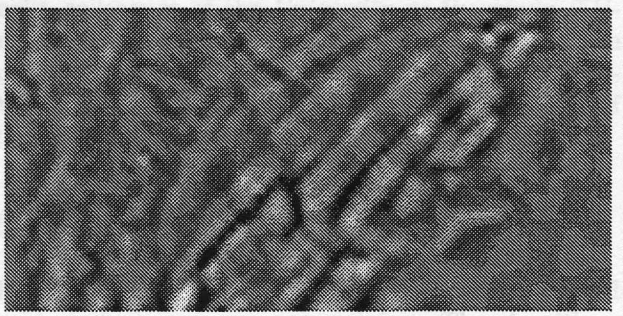

Figure 15: Detail image of levels 6 to 4 of image "Jura"

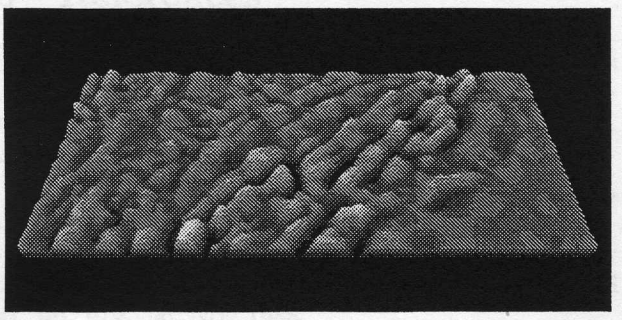

Figure 16: 3-D view of the details of levels 4 to 1 of image "Jura"

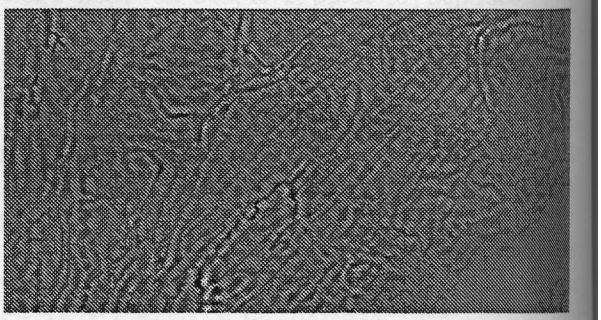

Figure 17: Détails of levels 4 to 1 of image "Jura"

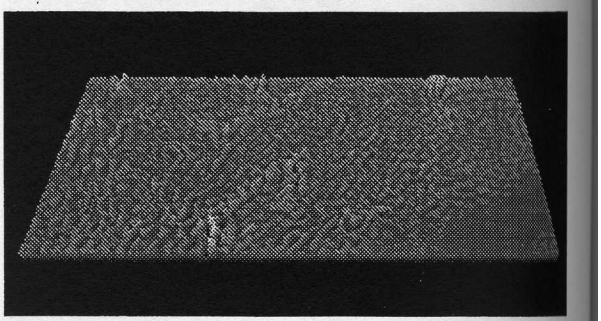

Figure 18: 3-D view of the details of levels 4 to 1 of the image "Jura"